

# Evolved tooth gain in sticklebacks is associated with a *cis*-regulatory allele of *Bmp6*

Phillip A. Cleves<sup>a</sup>, Nicholas A. Ellis<sup>a</sup>, Monica T. Jimenez<sup>a</sup>, Stephanie M. Nunez<sup>b,c,1</sup>, Dolph Schluter<sup>d</sup>, David M. Kingsley<sup>b,c</sup>, and Craig T. Miller<sup>a,2</sup>

<sup>a</sup>Department of Molecular and Cell Biology, University of California, Berkeley, CA 94720; <sup>b</sup>Department of Developmental Biology and <sup>c</sup>Howard Hughes Medical Institute, Stanford University, Stanford, CA 94305; and <sup>d</sup>Department of Zoology, University of British Columbia, Vancouver, Canada V6T 1Z4

Edited by Clifford J. Tabin, Harvard Medical School, Boston, MA, and approved August 7, 2014 (received for review April 25, 2014)

Developmental genetic studies of evolved differences in morphology have led to the hypothesis that *cis*-regulatory changes often underlie morphological evolution. However, because most of these studies focus on evolved loss of traits, the genetic architecture and possible association with *cis*-regulatory changes of gain traits are less understood. Here we show that a derived benthic freshwater stickleback population has evolved an approximate twofold gain in ventral pharyngeal tooth number compared with their ancestral marine counterparts. Comparing laboratory-reared developmental time courses of a low-toothed marine population and this high-toothed benthic population reveals that increases in tooth number and tooth plate area and decreases in tooth spacing arise at late juvenile stages. Genome-wide linkage mapping identifies largely separate sets of quantitative trait loci affecting different aspects of dental patterning. One large-effect quantitative trait locus controlling tooth number fine-maps to a genomic region containing an excellent candidate gene, *Bone morphogenetic protein 6* (*Bmp6*). Stickleback *Bmp6* is expressed in developing teeth, and no coding changes are found between the high- and low-toothed populations. However, quantitative allele-specific expression assays of *Bmp6* in developing teeth in F1 hybrids show that *cis*-regulatory changes have elevated the relative expression level of the freshwater benthic *Bmp6* allele at late, but not early, stages of stickleback development. Collectively, our data support a model where a late-acting *cis*-regulatory up-regulation of *Bmp6* expression underlies a significant increase in tooth number in derived benthic sticklebacks.

*Gasterosteus* | polyphyodonty | craniofacial | adaptation | quantitative genetics

Understanding the developmental genetic basis of morphological evolution is a long-standing goal in biology (1, 2). Evolved morphological differences can be “loss” (regressive) traits, where morphological features are lost or reduced, or “gain” (constructive) traits, where morphological features are gained or increased. Although many of the traits best understood at the molecular level involve loss traits (1, 2), recent studies have begun to genetically dissect some evolved gain traits (3–5). However, whether gain traits have similar genetic architectures as loss traits and whether gain traits are also associated with *cis*-regulatory changes remains largely unknown.

Teeth are a classic vertebrate model system for studying morphological evolution, due to their excellent preservation in the fossil record. Teeth are also a classic vertebrate model system for organogenesis, because teeth, like many other organs, develop through reciprocal signaling interactions between epithelia and mesenchyme. Continuing efforts have produced a rich understanding of the genetic networks that orchestrate tooth morphogenesis in model systems (6). However, despite the wealth of knowledge about tooth evolution and development, we still know little about the number and type of genetic changes that accompany diversification of dental patterning during evolution.

Pharyngeal jaws and teeth, used during mastication in fish, are located in the posterior branchial segments in the fish’s throat (7, 8). In teleost fish, pharyngeal jaw patterning is an adaptive trait

that covaries with diet and trophic niche (9). The rich phenotypic diversity of pharyngeal jaws and teeth in fish, coupled with the understanding of the genetic networks of tooth development from model organisms, offers an opportunity to understand the developmental genetic basis of evolved changes in tooth patterning.

The threespine stickleback (*Gasterosteus aculeatus*) fish has emerged as an excellent model system allowing for genetic dissection of evolutionary change in vertebrates (10). Sticklebacks have undergone an extensive adaptive radiation, independently colonizing thousands of freshwater lakes and creeks generated after widespread melting of glaciers at the end of the last ice age (11). The dietary shifts to larger prey accompanying freshwater adaptation have resulted in evolved changes in trophic morphology (12, 13). Despite striking morphological differences between marine and freshwater populations, hybrids are fertile, allowing forward genetic analysis of evolved differences. In several lakes, “species pairs” of benthic and limnetic stickleback morphs are found (13). In each of these lakes, a benthic species is adapted to feeding on macroinvertebrates in the littoral zone or deeper sediments. This derived diet differs from the diet of both the limnetic species and ancestral marine forms, both of which feed on smaller zooplankton. Benthic sticklebacks have evolved trophic adaptations matched for this specialized diet (13, 14). Here we describe evolved tooth gain, a heritable constructive increase in tooth number compared with ancestral marine

## Significance

How body pattern evolves in nature remains largely unknown. Although recent progress has been made on the molecular basis of losing morphological features during adaptation to new environments (regressive evolution), there are few well worked out examples of how morphological features may be gained in natural species (constructive evolution). Here we use genetic crosses to study how threespine stickleback fish have increased their tooth number in a new freshwater environment. Genetic mapping and gene expression experiments suggest regulatory changes have occurred in the gene for a bone morphogenetic signaling molecule, leading to increased expression in the freshwater fish that have more teeth. Our studies suggest that changes in gene regulation may underlie both gain and loss traits during vertebrate evolution.

Author contributions: P.A.C., N.A.E., D.S., D.M.K., and C.T.M. designed research; P.A.C., N.A.E., M.T.J., S.M.N., and C.T.M. performed research; P.A.C., N.A.E., M.T.J., S.M.N., D.S., D.M.K., and C.T.M. analyzed data; and P.A.C., D.S., D.M.K., and C.T.M. wrote the paper.

The authors declare no conflict of interest.

This article is a PNAS Direct Submission.

Data deposition: The DNA sequences reported in this paper have been deposited in the GenBank and Probe databases [accession nos. [KM406380–KM406383](#) (Genbank); [Pr032250564–Pr032250575](#), [Pr032250589–Pr032250592](#) (Probe)].

<sup>1</sup>Present address: University of Michigan School of Dentistry, Ann Arbor, MI 48109.

<sup>2</sup>To whom correspondence should be addressed. Email: [ctmiller@berkeley.edu](mailto:ctmiller@berkeley.edu).

This article contains supporting information online at [www.pnas.org/lookup/suppl/doi:10.1073/pnas.1407567111/-DCSupplemental](http://www.pnas.org/lookup/suppl/doi:10.1073/pnas.1407567111/-DCSupplemental).

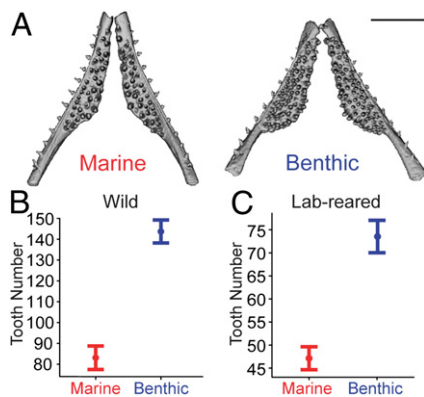


**Fig. 1.** Heritable evolved tooth gain in derived benthic fish. (A) MicroCT images of wild adult stickleback ventral pharyngeal tooth plates of marine fish from Rabbit Slough, Alaska (Left) and benthic fish from Paxton Lake, Canada (Right). (Scale bar, 1 mm.) (B and C) Total ventral pharyngeal tooth number in wild (B) and laboratory-reared (C) adults shows benthic fish have significantly higher tooth counts ( $P = 8.8 \times 10^{-7}$  and  $P = 4.9 \times 10^{-7}$  in two-tailed *t* tests for wild and laboratory-reared, respectively). Error bars are SEM.

fish, in a derived benthic stickleback population. We then apply quantitative genetics and developmental biology methods to begin to dissect the genetic and developmental basis of this evolved gain trait.

## Results

**Derived Benthic Fish Have Evolved Increases in Tooth Number.** Because benthic sticklebacks have undergone an adaptive shift in diet, and because aspects of pharyngeal jaw patterning correlate with trophic niche in other species (9), we hypothesized that wild benthic fish have evolved changes in tooth patterning compared with ancestral marine fish. To test this hypothesis, we first quantified adult ventral pharyngeal tooth number from wild benthic fish from Paxton Lake, Canada (PAXB, hereafter called “benthic”) and an ancestral marine population from Rabbit Slough, Alaska (RABS, hereafter called “marine”). In these samples, the wild benthic population has an approximate twofold gain in tooth number compared with wild marine adults (Fig. 1 *A* and *B* and *SI Appendix*, Table S1). To determine whether this striking difference in tooth number is heritable, we quantified tooth number in adult fish from each population in a common laboratory-reared environment. The increased tooth number in benthic fish compared with marine fish is also seen in laboratory-reared stocks fed the same diet (Fig. 1*C* and *SI Appendix*, Table S1), showing that the tooth number differences have a large heritable component.

**Evolved Changes in Tooth Patterning Occur Late in Development.** To examine when during development this evolved increase in tooth number appears, we generated a dense developmental time course of laboratory-reared fish from both marine and benthic populations and quantified tooth number (Fig. 2*A*). Tooth number between the two populations was not significantly different at early larval stages but began diverging when fish reached a total length of about 20 mm (Fig. 2*A*). Tooth number continued diverging after 20 mm, with benthic fish continuing to add new teeth while marine fish tooth number plateaus, resulting in the approximate twofold difference in tooth number seen in adults (Fig. 2*A* and *SI Appendix*, Table S2). The observed difference in tooth number between marine and benthic fish could arise either through an increase in the size of the tooth field and/or through an increased density of teeth in that field. We quantified tooth plate area (area of tooth-bearing portion of the fifth ceratobranchial bone) and average intertooth spacing throughout the developmental time courses. Relative to marine fish, in benthic fish tooth number and tooth plate area increased, while intertooth spacing decreased, with all three traits diverging late in development, after the 20-mm stage (Fig. 2*B* and *C* and *SI Appendix*, Table S2). Thus, the late increase in tooth number in derived benthic fish is accompanied by at least two other late developmental patterning changes: an expansion of the tooth field and an increase in tooth density within that field. These increases in tooth number and tooth plate area and decreased intertooth spaces were also observed in F1 marine by benthic hybrid fish, showing that the benthic phenotypes are at least partially dominant (*SI Appendix*, Table S3).

**Genome-wide Architecture of Evolved Changes in Tooth Number, Tooth Plate Area, and Spacing.** Previous work identified quantitative trait loci (QTL) controlling tooth number in a large genetic cross of 370 F2 fish derived from a Paxton benthic and a Japanese marine grandparent (15). Compared with Paxton benthic freshwater sticklebacks, Japanese marine sticklebacks, like Alaskan marine sticklebacks from the Rabbit Slough population, are low-toothed both in the wild and in the laboratory (*SI Appendix*, Table S1). To test whether tooth number, tooth plate area, and spacing are genetically separable traits, we measured tooth plate area and tooth spacing in 272 F2 progeny of the Japanese Marine  $\times$  Paxton benthic intercross. In the F2 progeny, tooth plate area and spacing are significantly correlated with tooth number; however, tooth plate area and intertooth spacing are not correlated with each other (*SI Appendix*, Fig. S1). These results were robustly replicated in a Paxton benthic  $\times$  Rabbit Slough marine F2 cross (*SI Appendix*, Fig. S1). Furthermore, a principal component analysis of these three tooth traits revealed that tooth plate area and spacing load orthogonally onto the first principal component (*SI Appendix*,

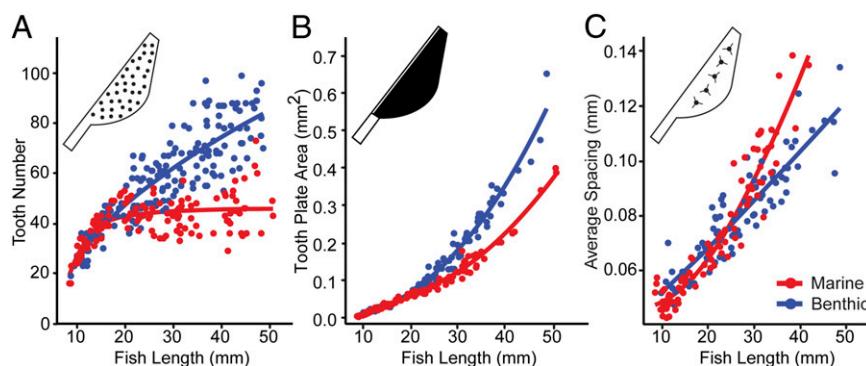


**Fig. 2.** Evolved differences in tooth number, area, and spacing appear late during development. Developmental time courses of laboratory-reared marine (red) and benthic (blue) fish of different total body lengths (*x* axis) for tooth number (A), tooth plate area (B), and tooth spacing (C). All three traits have diverged after 20-mm fish length.



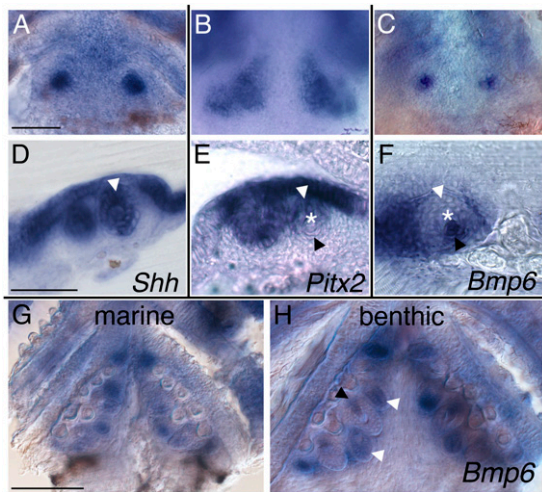


**Fig. 5.** *Bmp6* is expressed in developing stickleback teeth. Gene expression in developing benthic (A–F and H) and marine (G) stickleback teeth at 7.5 d postfertilization (dpf) (A–E) and 15 dpf (8 mm, F–H) revealed by in situ hybridization in whole-mount (A–C, G, and H) and 40- $\mu$ m vibratome sections of comparably staged developing tooth germs (D–F and SI Appendix, Fig. S4). (A–F) Tooth markers *Shh* (A and D) and *Pitx2* (B and E) are detected in the odontogenic epithelium, whereas *Bmp6* is expressed dynamically in odontogenic epithelium early (C and H) and in odontogenic mesenchyme in newly ossifying teeth (F and H). (G and H) *Bmp6* continues to be expressed in teeth later in development in both marine and benthic larvae. White arrowheads, odontogenic epithelium; asterisks, newly mineralized developing teeth; black arrowheads, odontogenic mesenchyme. (Scale bars, A–F = 50  $\mu$ m, G and H = 100  $\mu$ m.)

***cis*-Regulatory Changes Have Elevated Expression of the Benthic *Bmp6* Allele During Tooth Development.** We sequenced the exons of *Bmp6* in marine and benthic fish and found no nonsynonymous coding differences (SI Appendix, Fig. S7). To test for possible *cis*-acting regulatory differences in expression of marine and benthic alleles, we generated F1 hybrids between marine and benthic fish and used pyrosequencing assays to ask whether benthic and marine alleles made equal contributions to the overall level of *Bmp6* mRNA expression in F1 hybrid tooth plates. Allele-specific expression assays allow for the precise quantification of *cis*-regulatory differences between the two chromosomes in the same cells of the same fish in an identical *trans*-acting environment (31). We tested for a *cis*-regulatory change in *Bmp6* at three developmental time points, one before (larval), one during (juvenile), and one after (adult) the tooth number divergence. We detected no significant *cis*-regulatory difference in *Bmp6* at an early larval stage before the tooth number divergence in the time course (Fig. 6). However, in both juveniles and adults, when tooth number differences are first being established and are further diverging between marine and benthic populations, we detected a highly significant allele-specific expression difference, with  $\sim 1.4$ -fold up-regulation of *Bmp6* expression from the benthic allele in F1 hybrid fish (Fig. 6). This significant up-regulation of *Bmp6* at a later developmental stage mirrors both the late divergence in tooth number and the late-acting nature of the chromosome 21 QTL. These results support the hypothesis that a temporally regulated *cis*-regulatory difference in *Bmp6* expression drives the difference in tooth number between benthic and marine sticklebacks.

## Discussion

Our studies show that Paxton benthic freshwater sticklebacks have evolved major changes in tooth number, tooth plate area, and intertooth spacing that arise relatively late during development. Because sticklebacks, like most teleosts, retain the basal vertebrate condition of polyphyodonty (continuous tooth

replacement) (32), the late divergence in tooth number could result from a change in the rate of the tooth regeneration program late in development, once the initial tooth pattern has been established. This late-forming increase in tooth number may match the time period when benthic fish begin to benefit from increased tooth number (i.e., perhaps wild benthic larvae do not normally begin exploiting a benthic diet until about 20–25 mm in length). Alternatively, developmental or genetic constraints may lead to late-forming divergence. For example, altering the tooth developmental program at earlier stages may lead to deleterious pleiotropic consequences, or available standing genetic variation might primarily affect late, not early, development.

Although our laboratory-reared data show that major differences in tooth number are maintained between marine and freshwater fish when reared in a common laboratory environment, tooth numbers in both populations are reduced in laboratory-reared fish compared with wild fish. Differences in chronological age likely contribute to this difference, because wild fish are likely at least 1 y old, whereas our laboratory-reared adults were 6 mo old. In addition, tooth number may be influenced by diet and rearing conditions, as has previously been reported in cichlids (33).

Previous quantitative genetic studies of stickleback pharyngeal tooth number revealed five QTL controlling ventral pharyngeal tooth number in a F2 genetic cross between an ancestral low-toothed Japanese marine fish and a derived high-toothed Paxton benthic freshwater fish (15). Our more detailed studies suggest that differences in total adult tooth number arise from a combination of several factors, including changes in the development programs controlling tooth number, the size of the tooth field, and the spacing of teeth within that field. This conclusion is supported by the statistical relationships between tooth number, area, and spacing in the F2 cross and by the genome-wide linkage mapping results of all three phenotypes. We have identified at least seven QTL that have significant effects on tooth number, tooth plate size, or tooth spacing. Different QTLs affect one, two, or three different tooth phenotypes (tooth number, tooth spacing, and tooth plate size), showing modular control of evolved changes in dental patterning.

In other fish, pharyngeal jaw patterning is correlated with dietary niche, likely due to adaptive advantages of different morphologies in feeding success on different diets (9). Because benthic fish are well described as having trophic specializations for eating benthos (13), we hypothesize that the evolved tooth gain in benthic sticklebacks is also an adaptive trait that has been selected during an ecological shift to a benthic diet. We note that

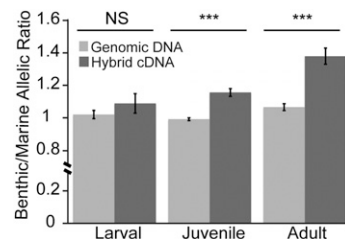


**Fig. 6.** *cis*-regulatory up-regulation of the benthic allele of *Bmp6* in late, not early, stages of tooth development. Shown are the ratios of benthic to marine alleles measured by pyrosequencing assays from either genomic DNA (light gray) or tooth plate cDNA (dark gray) from benthic  $\times$  marine F1 hybrids at three different developmental stages. No significant difference in *Bmp6* expression was detected between marine and benthic alleles at the larval stage, but at the juvenile and adult stage the benthic allele was significantly up-regulated (sample sizes and *P* values by the Wilcoxon signed rank test for early, juvenile, and adult are  $n = 12$ ,  $P = 0.27$ ;  $n = 18$ ,  $P = 0.0003$ ; and  $n = 13$ ,  $P = 0.0005$ , respectively). Error bars are SEM.

of the seven tooth-patterning QTL, only three go in a direction that is concordant with the overall shift in tooth number in the parental populations (i.e., benthic alleles conferring more teeth) based on the developmental time courses. However, the QTL with the largest phenotypic effect on chromosome 21 does act in a direction that is consistent with the overall trend in tooth number in the parental populations (benthic allele conferring more teeth). Perhaps the smaller-effect QTL that have effects in the opposite direction result from chromosome 21's effect overshooting the adaptive peak for tooth patterning in this recently evolved population, with other loci evolving to bring tooth patterning closer to the adaptive peak (34). The mixed direction of effects of benthic alleles could alternatively result from pleiotropy (35), with QTL controlling other adaptive benthic phenotypes that might secondarily affect tooth patterning. For example, the large-effect tooth-spacing QTL on chromosome 4 overlaps the *Ectodysplasin* (*Eda*) gene which controls adaptive reductions in armor plate patterning (36) and is also well known to affect vertebrate tooth patterning (37, 38). Interestingly, *Eda* also plays a role in the spacing of hair placodes and tooth cusps in mice (39, 40), making *Eda* an excellent candidate for underlying the tooth-spacing QTL on chromosome 4. A third possibility is that some or all of these tooth traits could be changing due to genetic drift occurring after freshwater colonization. As several other species pairs and hundreds of other freshwater populations with trophic modifications have been described (12, 13, 41–43), one test of adaptive significance will be to ask whether other derived benthic lake or creek freshwater stickleback populations have also evolved increases in tooth number. Molecular genetic identification of the tooth-patterning QTL that are segregating in the current cross, combined with population genetic tests of molecular variation surrounding causal loci, should also help distinguish these models.

To begin to study the molecular mechanisms behind evolved tooth gain, we fine-mapped the largest-effect tooth number QTL on chromosome 21. A previous study identified a cluster of QTL on chromosome 21 controlling several derived freshwater skeletal traits (15). This QTL cluster mapped near a large genomic inversion previously shown to display strong worldwide patterns of divergence between marine and freshwater populations (44), suggesting that multiple phenotypes may be controlled by linked genetic changes within the chromosome inversion. Interestingly, we find that the 1.5-LOD candidate interval for the chromosome 21 tooth QTL maps over 1.5 Mb from the inversion, strongly suggesting that the molecular changes driving tooth gain map outside the inverted region.

The new fine-mapped interval for the tooth QTL contains an excellent candidate gene, *Bmp6*. We show that *Bmp6* is expressed in developing teeth in marine and benthic sticklebacks, has no predicted coding changes between populations, but has a late-onset *cis*-regulatory up-regulation in benthic fish. Because in other vertebrates, BMPs act as activators of tooth development (45), we hypothesize that the elevated *Bmp6* expression observed in benthic sticklebacks contributes to their increased tooth number controlled by the chromosome 21 region. Bone Morphogenetic Proteins were originally identified based on their remarkable ability to induce ectopic bone when implanted at new sites in animals (46). Thus, increases in tooth plate area could also result from increased *Bmp6* expression. The divergence in tooth number and *Bmp6* *cis*-regulation at late, not early, developmental stages might reflect a heterochronic shift in the benthic population, where the benthic tooth development and replacement program is “stuck” in the early rapid tooth-generating phase observed in early larval stages in both marine and benthic fish. Although we parsimoniously favor the hypothesis that *Bmp6* underlies the evolved differences in tooth number, tooth plate area, and intertooth spacing, we note that the fine mapping was only done for tooth number, so it is possible that other genes underlie the evolved changes in tooth plate area and intertooth spacing.

The use of BMP ligands as major drivers of morphological evolution in vertebrates is striking. BMP family members have been implicated in several vertebrate evolved traits: size and shape of the beak in Darwin's finches, size and shape of the jaw in cichlids, jaw and skull variation in brachycephalic dogs, and avian feather patterning (47–50). Although based on a limited number of reported cases and possibly affected by ascertainment biases, this apparent reuse of the same signaling pathway across taxa may reflect a predisposition for *Bmp* genes to be used during morphological evolution, perhaps due to having complex, modular *cis*-regulatory architecture to generate evolutionary variation (51, 52).

Previous QTL mapping studies in sticklebacks have shown that major changes in pelvic hindfin development, armor plate formation, and body pigmentation are all due to alterations in key developmental signaling molecules and transcription factors (36, 53–55). In each of these previous cases, freshwater fish have evolved a major loss or reduction of skeletal structures that were originally present in marine ancestors. In all three cases, *cis*-regulatory changes are implicated, either directly (53, 54) or inferred (36). Here we show that a major gain in tooth number can also be genetically mapped to a relatively small number of chromosome regions. The QTLs with largest effects on tooth number control somewhat less of the overall variance than the previously identified QTL for armor plates, pelvis, and pigment (each of which controls 50% or more of the variance in the corresponding trait). Nevertheless, the overall effects of the tooth-patterning QTLs are still quite large compared with classical predictions of nearly infinitesimal effects for genetic changes underlying evolved differences in natural populations. Finally, our results with *Bmp6* show that for both loss and gain traits, the chromosome regions with largest phenotypic effects show clear evidence of *cis*-acting regulatory changes in key developmental control genes. Although many more case studies will be needed to draw general conclusions, collectively, these studies suggest that similar general principles may underlie the evolution of both loss and gain traits and that regulatory changes in developmental control genes play an important role in both regressive and constructive evolution of the vertebrate skeleton.

## Materials and Methods

**Stickleback Husbandry.** Lab-reared fish were raised in 110-liter tanks under common conditions (3.5 g/l Instant Ocean salt, 0.4 mL/l NaHCO<sub>3</sub>) and fed live brine shrimp as larvae, then frozen daphnia, bloodworms, and Mysis shrimp as juveniles and adults. All experiments and field collections were done with the approval of the Institutional Animal Care and Use Committee from University of California, Berkeley, Stanford University, or the University of British Columbia.

**QTL Mapping.** QTL mapping was done using R/qtl (56). To map QTL for adult tooth number, area, and spacing, we analyzed a subset ( $n = 272$  fish) of a previously described (16) Paxton Benthic and Japanese Marine F2 cross. Two hundred seventy-five microsatellite markers were genotyped in each F2. Tooth number, area, and spacing were quantified in each F2. As all three traits were significantly correlated with fish total length, residuals from a linear regression were used for each of the three traits. See *SI Appendix, SI Materials and Methods*, for details of QTL mapping.

**In Situ Hybridization.** Marine and benthic embryos and larvae were euthanized, fixed overnight in 4 g paraformaldehyde in 100 ml 1×PBS, then dehydrated and stored at  $-20^{\circ}\text{C}$  in methanol. For larvae older than 9 d postfertilization, ventral tooth plates were dissected after rehydration from methanol and before in situ hybridization. In situ hybridization was performed essentially as described (57) but with in situ done in tubes in a water bath not baskets and using a 2-d hybridization for older larval stages. For sections, whole-mount in situ were fixed overnight in 4 g paraformaldehyde in 100 ml 1× PBS, embedded in gelatin–albumin cross-linked with 1.75% glutaraldehyde, and sectioned at 40  $\mu\text{m}$  on a Pelco 101 Vibratome Series 1000. Primer sequences for generating the clones used to make the *Bmp6*, *Shh*, *Pitx2*, and *Tfap2a* riboprobes are listed in *SI Appendix*.

**Pyrosequencing of F1 Hybrids.** For allele-specific expression experiments, Paxton benthic freshwater fish were crossed with Rabbit Slough marine fish by in vitro fertilization to generate hybrid F1s. The bilateral pair of ventral pharyngeal tooth plates from each hybrid was dissected on ice from larval, juvenile, and adult stages (~10–20 mm,  $n = 12$ ; ~25–40 mm,  $n = 18$ ; and >40 mm in total length,  $n = 13$ , respectively). See *SI Appendix* for primer sequences used for RT-PCR and pyrosequencing and additional methods.

**ACKNOWLEDGMENTS.** We thank Mike Bell and Brian Summers for generously providing wild adult RABS fish, Priscilla Erickson for generating some

of the lab-reared PAXB fish, Andrew Glazer for generating the *Shh* probe, and Gareth Fraser and Peter Walentek for useful suggestions on sectioning. This work was supported in part by National Science Foundation Graduate Research Fellowships (to P.A.C. and N.A.E.); National Institutes of Health Genetics Training Grant 5T32GM007127 (to P.A.C.); an Achievement Rewards for College Scientists fellowship (to N.A.E.); a Canada Research Chair and grants from Natural Sciences and Engineering Research Council and the Canada Foundation for Innovation (to D.S.); an NIH Center for Excellence in Genomic Studies grant (5P50HG2568) and investigator position at the Howard Hughes Medical Institute (to D.M.K.); and a March of Dimes Basil O'Connor award, the Pew Charitable Trusts, and NIH R01-DE021475 (to C.T.M.).

- Carroll SB (2008) Evo-devo and an expanding evolutionary synthesis: A genetic theory of morphological evolution. *Cell* 134(1):25–36.
- Stern DL (2000) Evolutionary developmental biology and the problem of variation. *Evolution* 54(4):1079–1091.
- Protas M, et al. (2008) Multi-trait evolution in a cave fish, *Astyanax mexicanus*. *Evol Dev* 10(2):196–209.
- Wark AR, et al. (2012) Genetic architecture of variation in the lateral line sensory system of threespine sticklebacks. *G3* 2(9):1047–1056.
- Werner T, Koshikawa S, Williams TM, Carroll SB (2010) Generation of a novel wing colour pattern by the Wingless morphogen. *Nature* 464(7292):1143–1148.
- Jernvall J, Thesleff I (2012) Tooth shape formation and tooth renewal: Evolving with the same signals. *Development* 139(19):3487–3497.
- Lauder GV (1983) Functional design and evolution of the pharyngeal jaw apparatus in euteleostean fishes. *Zool J Linn Soc-Lond* 77(1):1–38.
- Wainwright PC (2005) Functional morphology of the pharyngeal jaw apparatus. *Biomechanics of Fishes*, eds Shadwick R, Lauder GV (Academic Press, New York), pp 77–101.
- Muschick M, Indermaur A, Salzburger W (2012) Convergent evolution within an adaptive radiation of cichlid fishes. *Curr Biol* 22(24):2362–2368.
- Kingsley DM, Peichel CL (2007) The molecular genetics of evolutionary change in sticklebacks. *Biology of the Three-Spine Stickleback*, eds Ostlund-Nilsson S, Mayer I, Huntingford FA (CRC Press, Boca Raton), pp 41–81.
- Bell MA, Foster SA (1994) *The Evolutionary Biology of the Threespine Stickleback* (Oxford Univ Press, Oxford, U. K.), 571 pp.
- Caldecutt WJ, Bell MA, Buckland-Nicks JA (2001) Sexual dimorphism and geographic variation in dentition of threespine stickleback, *Gasterosteus aculeatus*. *Copeia* (4):936–944.
- Schluter D, McPhail JD (1992) Ecological character displacement and speciation in sticklebacks. *Am Nat* 140(1):85–108.
- McPhail JD (1992) Ecology and evolution of sympatric sticklebacks (*Gasterosteus*): Evidence for a species pair in Paxton Lake, Texada Island, British Columbia. *Can J Zool* 70:361–369.
- Miller CT, et al. (2014) Modular skeletal evolution in sticklebacks is controlled by additive and clustered quantitative trait loci. *Genetics* 197(1):405–420.
- Colosimo PF, et al. (2004) The genetic architecture of parallel armor plate reduction in threespine sticklebacks. *PLoS Biol* 2(5):E109.
- Andl T, et al. (2004) Epithelial Bmpr1a regulates differentiation and proliferation in postnatal hair follicles and is essential for tooth development. *Development* 131(10):2257–2268.
- Bei M, Kratochwil K, Maas RL (2000) BMP4 rescues a non-cell-autonomous function of *Msx1* in tooth development. *Development* 127(21):4711–4718.
- Fraser GJ, Bloomquist RF, Streelman JT (2013) Common developmental pathways link tooth shape to regeneration. *Dev Biol* 377(2):399–414.
- Jia S, et al. (2013) Roles of Bmp4 during tooth morphogenesis and sequential tooth formation. *Development* 140(2):423–432.
- Vainio S, Karavanova I, Jowett A, Thesleff I (1993) Identification of BMP-4 as a signal mediating secondary induction between epithelial and mesenchymal tissues during early tooth development. *Cell* 75(1):45–58.
- Wang Y, et al. (2012) BMP activity is required for tooth development from the lamina to bud stage. *J Dent Res* 91(7):690–695.
- Bitgood MJ, McMahon AP (1995) Hedgehog and Bmp genes are coexpressed at many diverse sites of cell-cell interaction in the mouse embryo. *Dev Biol* 172(1):126–138.
- Fraser GJ, Berkovitz BK, Graham A, Smith MM (2006) Gene deployment for tooth replacement in the rainbow trout (*Oncorhynchus mykiss*): A developmental model for evolution of the osteichthyan dentition. *Evol Dev* 8(5):446–457.
- Fraser GJ, Graham A, Smith MM (2004) Conserved deployment of genes during odontogenesis across osteichthyans. *Proc Biol Sci* 271(1555):2311–2317.
- Mucchielli ML, et al. (1997) Mouse *Otx2/RIEG* expression in the odontogenic epithelium precedes tooth initiation and requires mesenchyme-derived signals for its maintenance. *Dev Biol* 189(2):275–284.
- Aberg T, Wozney J, Thesleff I (1997) Expression patterns of bone morphogenetic proteins (Bmps) in the developing mouse tooth suggest roles in morphogenesis and cell differentiation. *Dev Dyn* 210(4):383–396.
- Fraser GJ, et al. (2009) An ancient gene network is co-opted for teeth on old and new jaws. *PLoS Biol* 7(2):e31.
- O'Connell DJ, et al. (2012) A Wnt-bmp feedback circuit controls intertissue signaling dynamics in tooth organogenesis. *Sci Signal* 5(206):ra4.
- Wise SB, Stock DW (2006) Conservation and divergence of Bmp2a, Bmp2b, and Bmp4 expression patterns within and between dentitions of teleost fishes. *Evol Dev* 8(6):511–523.
- Wittkopp PJ (2011) Using pyrosequencing to measure allele-specific mRNA abundance and infer the effects of cis- and trans-regulatory differences. *Methods Mol Biol* 772:297–317.
- Huysseune A, Witten PE (2006) Developmental mechanisms underlying tooth patterning in continuously replacing osteichthyan dentitions. *J Exp Zool B Mol Dev Evol* 306(3):204–215.
- Huysseune A (1995) Phenotypic plasticity in the lower pharyngeal jaw dentition of *Astatotrochomis alluaudi* (Teleostei: Cichlidae). *Arch Oral Biol* 40(11):1005–1014.
- Orr HA (2005) The genetic theory of adaptation: A brief history. *Nat Rev Genet* 6(2):119–127.
- Rogers SM, et al. (2012) Genetic signature of adaptive peak shift in threespine stickleback. *Evolution* 66(8):2439–2450.
- Colosimo PF, et al. (2005) Widespread parallel evolution in sticklebacks by repeated fixation of Ectodysplasin alleles. *Science* 307(5717):1928–1933.
- Aigler SR, Jandzik D, Hatta K, Uesugi K, Stock DW (2014) Selection and constraint underlie irreversibility of tooth loss in cypriniform fishes. *Proc Natl Acad Sci USA* 111(21):7707–7712.
- Häärä O, et al. (2012) Ectodysplasin regulates activator-inhibitor balance in murine tooth development through Fgf20 signaling. *Development* 139(17):3189–3199.
- Harjunmaa E, et al. (2012) On the difficulty of increasing dental complexity. *Nature* 483(7389):324–327.
- Mustonen T, et al. (2004) Ectodysplasin A1 promotes placodal cell fate during early morphogenesis of ectodermal appendages. *Development* 131(20):4907–4919.
- Gross HP, Anderson JM (1984) Geographic variation in the gillrakers and diet of European threespine sticklebacks, *Gasterosteus aculeatus*. *Copeia* (1):87–97.
- Hagen DW, Gilbertson LG (1972) Geographic variation and environmental selection in *Gasterosteus aculeatus L* in Pacific Northwest, America. *Evolution* 26(1):32–51.
- McPhail JD (1993) Ecology and evolution of sympatric sticklebacks (*Gasterosteus*): Origin of the species pairs. *Can J Zool* 71(3):515–523.
- Jones FC, et al. (2012) The genomic basis of adaptive evolution in threespine sticklebacks. *Nature* 484(7392):55–61.
- Kavanagh KD, Evans AR, Jernvall J (2007) Predicting evolutionary patterns of mammalian teeth from development. *Nature* 449(7161):427–432.
- Reddi AH, Reddi A (2009) Bone morphogenetic proteins (BMPs): From morphogens to metabologens. *Cytokine Growth Factor Rev* 20(5–6):341–342.
- Abzhanov A, Protas M, Grant BR, Grant PR, Tabin CJ (2004) Bmp4 and morphological variation of beaks in Darwin's finches. *Science* 305(5689):1462–1465.
- Albertson RC, Streelman JT, Kocher TD, Yelick PC (2005) Integration and evolution of the cichlid mandible: The molecular basis of alternate feeding strategies. *Proc Natl Acad Sci USA* 102(45):16287–16292.
- Mou C, et al. (2011) Cryptic patterning of avian skin confers a developmental facility for loss of neck feathering. *PLoS Biol* 9(3):e1001028.
- Schoenebeck JJ, et al. (2012) Variation of BMP3 contributes to dog breed skull diversity. *PLoS Genet* 8(8):e1002849.
- Guenther C, Pantalena-Filho L, Kingsley DM (2008) Shaping skeletal growth by modular regulatory elements in the Bmp5 gene. *PLoS Genet* 4(12):e1000308.
- Kingsley DM (1994) What do BMPs do in mammals? Clues from the mouse short-ear mutation. *Trends Genet* 10(1):16–21.
- Chan YF, et al. (2010) Adaptive evolution of pelvic reduction in sticklebacks by recurrent deletion of a Pitx1 enhancer. *Science* 327(5963):302–305.
- Miller CT, et al. (2007) cis-regulatory changes in Kit ligand expression and parallel evolution of pigmentation in sticklebacks and humans. *Cell* 131(6):1179–1189.
- Shapiro MD, et al. (2004) Genetic and developmental basis of evolutionary pelvic reduction in threespine sticklebacks. *Nature* 428(6984):717–723.
- Broman KW, Sen S (2009) *A Guide to QTL Mapping with R/qtl* (Springer, New York).
- Thisse C, Thisse B (2008) High-resolution in situ hybridization to whole-mount zebrafish embryos. *Nat Protoc* 3(1):59–69.

## SI Appendix

### Evolved tooth gain in sticklebacks is associated with a cis-regulatory allele of *Bmp6*

Phillip A. Cleves<sup>1</sup>, Nicholas A. Ellis<sup>1</sup>, Monica T. Jimenez<sup>1</sup>, Stephanie M. Nunez<sup>2,3</sup>, Dolph Schluter<sup>4</sup>, David M. Kingsley<sup>2</sup>, Craig T. Miller<sup>1</sup>

<sup>1</sup>Department of Molecular and Cell Biology, University of California-Berkeley, Berkeley CA, 94720, USA

<sup>2</sup>Department of Developmental Biology and Howard Hughes Medical Institute, Stanford University, Stanford, CA, 94305, USA

<sup>3</sup>present address = University of Michigan School of Dentistry, Ann Arbor, MI, 48109, USA

<sup>4</sup>Department of Zoology, University of British Columbia, Vancouver, Canada V6T 1Z4

This SI file includes:

Supplemental Materials and Methods and References

Supplementary Tables 1-5

Supplementary Figures 1-7

## Supplemental Materials and Methods

### Skeletal morphology visualization and quantification

Adult lab-reared fish were fixed in 4% paraformaldehyde overnight, washed in H<sub>2</sub>O, stained with 0.008% Alizarin Red in 1% KOH overnight, washed in H<sub>2</sub>O, then cleared in 50% glycerol and 0.25% KOH. Branchial skeletons were dissected, cleared, and mounted, and Alizarin Red fluorescent teeth were quantified on a DM2500 Leica microscope using a TX2 filter. Significant differences between the populations in both lab and wild datasets were tested using two-tailed *t* tests. Wild PAXB and RABS fish, and F2 chromosome 21 recombinants from the PAXB x JAMA F2 cross were scanned unstained in ethanol using a Scanco uCT40 microcomputerized tomographer at 55 kVp at high resolution, averaging four frames, and teeth counted from digital volumes of ventral pharyngeal tooth plates.

For time courses, total fish length was measured after overnight fixation in 4% paraformaldehyde. Fish at different stages were stained with Alcian Blue and Alizarin Red stained using 100mM MgCl<sub>2</sub> as described (1) or only with 0.008% Alizarin Red in 1% KOH and then dissected, mounted, and total (left plus right) ventral pharyngeal tooth number quantified as above. For both the area and spacing measurements, grayscale images of Alizarin red fluorescence of bilateral ventral tooth plates were acquired with a DFC340 FX camera on a Leica M165FC dissecting microscope using a rhodamine filter. The periphery of the tooth plates for both left and right sides was outlined excluding teeth not connected to the tooth plate and area was calculated using ImageJ. The average area for both plates is shown. The spacing measurements were calculated by placing a landmark on each tooth position on the left/right ventral pharyngeal tooth plate and measuring the distance to the closest three neighboring teeth using ImageJ and a custom Python script. The average of the bilateral spacing measurements is presented. Animals were only included in the spacing and area analysis if clear measurements could be made.

### QTL mapping tooth number, tooth plate area, and tooth spacing

We performed *scanone* in R/qtl (2) with Haley-Knott regressions to initially map QTL. For each phenotype, we performed one thousand permutations with *scantwo* to calculate the trait-specific LOD threshold at which  $\alpha = 0.05$ . Conservatively, we used the highest of these LOD thresholds (4.1) for the significance threshold for all 3 traits. A forward-backward search was performed with *stepwiseqtl* to iteratively identify significant QTL with a main penalty of 4.1 and to identify the best fitting QTL model. Each QTL identified using *scanone* was also detected using *stepwiseqtl*. We calculated peak LOD and position for each QTL using *refineqtl* and percent variance explained with *fitqtl*. The LOD scores for chromosomes that did not have a significant effect in Figure 3 were determined with *addqtl*.

## Fine mapping tooth number QTL

To fine map the chromosome 21 tooth QTL, 1004 F2s from four additional families from the initial mapping cross were genotyped for the two-LOD boundary markers (Stn484 and Stn491) of the initial chromosome 21 tooth QTL to screen for recombinants. All recombinants were then genotyped for a set of polymorphic microsatellite markers (Table S5) across the QTL interval. These combined genotypes were used to make a linkage map for chromosome 21 with JoinMap 4.0 (Kyazma). The effects of fish size and family on total ventral pharyngeal tooth number were corrected for using a linear model in R ([www.r-project.org](http://www.r-project.org)). In the two largest families, the effects of genotypes at two previously described unlinked tooth number QTL (3) on chromosomes 4 and 20 were corrected for using *fitqtl* and genotypes at Gac4174 and Stn183 (chromosome 4) and Stn340 (chromosome 20). QTL mapping was done in the pooled dataset using *scanone* followed by *refineqtl* and *fitqtl*. *scanone* was used to perform 1000 simulations to calculate the LOD threshold (2.2) at which  $\alpha = 0.05$ . Gene content of the 2.56 Mb fine mapping interval was determined by counting genes predicted by either the ENSEMBL gene prediction or tBLASTn human protein track on the UCSC genome browser (<http://genome.ucsc.edu/>) for the interval between chromosome 21: 2,564,997-5,120,542 base pairs in the stickleback genome assembly (4).

## Mapping QTL in developmental time points of F2 cross

Lab-reared Paxton benthic (British Columbia, Canada) and Rabbit Slough (Alaska) fish were crossed by artificial fertilization and the F1s were intercrossed to generate F2s. F2s were sacrificed at 80 days post fertilization (dpf), 120 dpf, and adults (total n=142). These F2s were genotyped for the PAXB x JAMA F2 cross peak marker Stn489 (see Table S5 for primer sequences). The analyzed PAXB x RABS F2s total lengths ranged from 18-44mm. Animals were binned into three total length bins ranges so there were approximately equal numbers of animals in each bin (n=47-48) to compare across developmental time points. For the middle, but not early or late time points, tooth number significantly fit a linear regression to fish total length, so this effect was corrected for by taking the residuals of a linear regression to fish total length, followed by back-transforming values to fish with a length of 26.5 mm, the midpoint of the length bin. Effects of chromosome 21 genotype were tested using a one-way ANOVA in R.

## *Bmp6* sequencing

The seven predicted exons of *Bmp6* were amplified using RT-PCR from PAXB and RABS adult tooth plate cDNA using 5' UTR forward primer 5'-CTGCAGCTCCAAGAGAGACC -3' and 3'UTR reverse primer 5'-CTTTGCAAACCCCAACTTGT -3'. These primers amplified a ~1.3 kb PCR product, which was gel extracted (Qiagen kit) and sequenced, resulting in the predicted coding sequence shown in Fig. S7. To generate full exonic sequences of *Bmp6* from the different populations, the identified exons were PCR amplified from genomic DNA from PAXB, JAMA, and RABS fish. The reaction profile was 95°C for 3 m, 34 cycles of 95°C for 15 s, 56°C for 15 s, and 72°C for 30 s,

followed by 3 m at 72°C. The PCR fragments were purified using PCR purification kit (Qiagen) and sequenced. The primers used were: exon 1 5'-TAAGGGACTGCAGCTCCAAG-3' and 5'-GAAGTTCAACGATGACGATT-3'; exon 2 5'-GTGTGTGTTTCCATGCCACAG-3' and 5'-GAATCCACTCAAAGCTTCTT-3'; exon 3 5'-AAGTTGGGCTGCAGTTGTTT-3' and 5'-CGCGTGAGCTGGATCTCTTA-3'; exon 4 5'-CAACCTGTGGGTGATGAGC-3' and 5'-TCCTCTGTGCAACGAACTG-3'; exon 5 5'-CTCCGAGCCTCTCTCTAGCA-3' and 5'-TCATATGCGTCAGAGGATGG-3'; exon 6 5'-GCAGTTTGTTCATCCAGCTGTT-3' and 5'-AAGTCATGGCAAAGACGTG-3'; exon 7 5'-CTCGCTATACCAAACGTGAC-3' and 5'-GATTTAAACCGGGAGTCTAGC-3'. Genbank accession numbers of *Bmp6* sequences from Rabbit Slough and Paxton benthic mRNA and genomic DNA are KM406380-KM406383.

### Riboprobe design and synthesis

The plasmids used to synthesize the *Bmp6*, *Pitx2*, and *Shh* riboprobes were made by cloning RT-PCR amplicons into pBSII-SK+, amplified off random hexamer primed cDNA made from RNA of newly hatched (~8.5 dpf) Little Campbell marine fry. Amplicons were amplified with the following primers (with added 5' restriction enzyme cut sites underlined): *Bmp6* (~700bp) 5'-GCCGCTCGAGATGAACAGCTGCTGGCTTG-3' and 5'-GCCGTCTAGACTCATCACCCACAGGTTGC-3', *Pitx2* (~750bp) 5'-GCCGTCTAGACCTCAGTAACCCGTCTCTCAA-3' and 5'-GCCGGGGCCCAAGCAGGCCTGGGTTTCAT-3', *Shh* (~720bp) 5'-GCCGCTCGAGCGGGAGCAAATGAGACCTA-3' and 5'-GCCGTCTAGAATGCAGACATGAGGCAGAAT-3'. Resulting amplicons for each gene were then digested with XhoI and XbaI (*Bmp6* and *Shh*) or XbaI and ApaI (*Pitx2*) to generate sticky ends to directionally clone into pBSII-SK(+). The resultant plasmids were linearized with XhoI (*Bmp6* and *Shh*) or XbaI (*Pitx2*) and antisense riboprobes transcribed using T3 polymerase for the *Bmp6* and *Shh* probes or T7 polymerase for the *Pitx2* probe. The plasmid used to make the *Tfap2a* riboprobe was generated by first using the primers 5'-ATGGGAACTATTGCCAGCAC-3' and 5'-ACGAAGCGAAAAGAGGATGA-3' to amplify a ~760 bp amplicon by PCR off Little Campbell marine genomic DNA which was then TOPO TA (Invitrogen) cloned into pCR2.1. The resultant plasmid was linearized with HindIII and antisense riboprobe transcribed with T7 polymerase. ProbeDB sequences for *Bmp6*, *Pitx2*, *Shh*, and *Tfap2* riboprobes are Pr032250589, Pr032250590, Pr032250591, and Pr032250592, respectively.

### References

- (1) Walker MB & Kimmel CB (2007) A two-color acid-free cartilage and bone stain for zebrafish larvae. *Biotechnic & Histochemistry* 82(1):23-28.

- (2) Broman KW & Sen S (2009) *A Guide to QTL Mapping with R/qtl* (Springer, New York).
- (3) Miller CT, *et al.* (2014) Modular Skeletal Evolution in Sticklebacks Is Controlled by Additive and Clustered Quantitative Trait Loci. *Genetics* 197(1):405-20.
- (4) Jones FC, *et al.* (2012) The genomic basis of adaptive evolution in threespine sticklebacks. *Nature* 484(7392):55-61.

## Supplementary Tables

**Table S1. Wild and lab-reared tooth numbers of marine and freshwater fish**

	Population	Sample size	Mean standard length (mm)	Mean total tooth number	Comparison	<i>P</i> value
Wild	RABS	8	73.3 (1.4)	83 (16)	RABS-PAXB	< 0.00001
	JAMA	8	82.1 (2.5)	81 (19.7)	JAMA-RABS	0.98
	PAXB	20	58.0 (8.4)	144 (24.6)	PAXB-JAMA	< 0.00001
Lab-reared	RABS	21	38.8 (2)	47 (11.4)	RABS-PAXB	< 0.0001
	JAMA	23	38.5 (2.3)	58 (9.5)	JAMA-RABS	0.006
	PAXB	13	35.7 (1.4)	74 (12.7)	PAXB-JAMA	0.0004

Mean standard length in millimeters (mm) and total ventral pharyngeal tooth numbers with standard deviation (SD) for each are shown for Rabbit Slough marine (RABS), Japanese marine (JAMA), and Paxton benthic freshwater (PAXB) fish. *P* values from a Tukey's post-hoc test after an ANOVA for each population comparison are shown. The PAXB and RABS phenotypes are presented in Figure 1.

**Table S2. Divergence in tooth traits during development**

TL range	Trait	Sample size	Marine	Benthic	<i>P</i> value
8-20mm					
	Tooth Number	94	0.60 (3.75)	-0.65 (4.04)	0.12
	Tooth Plate Area	59	8.24E-05 (0.004)	-0.0003 (0.005)	0.76
	Tooth Spacing	58	-0.001 (0.004)	0.002 (0.006)	0.02
20-30mm					
	Tooth Number	83	-7.24 (6.6)	3.89 (8.8)	6.91E-08
	Tooth Plate Area	62	-0.019 (0.013)	0.014 (0.019)	2.86E-10
	Tooth Spacing	59	2.58E-05 (0.008)	-1.77E-05 (0.008)	0.98
30-57mm					
	Tooth Number	126	-17.34 (8.7)	11.04 (10.7)	4.9E-31
	Tooth Plate Area	55	-0.051 (0.031)	0.045 (0.038)	3.97E-14
	Tooth Spacing	50	0.009 (0.012)	-0.006 (0.009)	9.27E-06

For each tooth trait, mean size-corrected phenotypic value with standard deviation (SD) for each population (marine = RABS, benthic = PAXB) at three total length (TL) ranges is shown after fish size was adjusted for using a linear model in R. *P* values from an ANOVA for population effect are shown.

**Table S3. Tooth number, area, and spacing of marine by benthic F1 hybrids**

Trait	Sample Size	Marine	F1 Hybrid	Benthic	<i>P</i> values
Tooth Number	52,31,89	-18.06 (8.53)	4.92 (7.52)	8.84 (10.57)	<0.00001, 0.12
Tooth Plate Area	28,27,37	-0.057 (0.033)	0.022 (0.037)	0.027 (0.042)	<0.00001, 0.86
Tooth Spacing	25,29,38	0.01 (0.012)	-0.004 (0.013)	-0.003 (0.009)	0.00005, 0.91

For each tooth trait, mean size-corrected phenotypic value with standard deviation (SD) is presented for each population (marine = RABS, F1 Hybrids = PAXB x RABS F1, benthic = PAXB). Sample sizes for marine, F1s, and benthic classes respectively are listed in "Sample Size" column. Animals from the benthic and marine time courses were selected to overlap the Hybrid F1 total length range (28-50mm). Fish size was adjusted for using a linear model in R. *P* values from Tukey's posthoc test after an ANOVA are presented for the F1 hybrid comparisons to marine and benthic fish, respectively.

**Table S4. Location and effect of Tooth Pattern QTL**

Trait	LG	cM	Marker	LOD	MM	MB	BB	PVE
Tooth Number	4	60.4	Stn418	7.6	5.69	-0.52	-3.75	6.0
Tooth Number	10	11.7	Stn310	4.3	1.35	0.87	-3.80	3.3
Tooth Number	13	4.7	Stn153	6.0	-3.92	-0.05	3.39	4.6
Tooth Number	20	22.3	Gac1125	6.7	6.05	-1.39	-6.86	5.6
Tooth Number	21	4.0	Stn422	31.8	-9.93	-1.12	12.04	31.5
Tooth Spacing	4	57.0	Stn183	9.5	-0.013	-0.001	0.013	13.8
Tooth Spacing	21	3.2	Stn421	5.3	0.007	0.002	-0.010	7.3
Tooth Plate Area	1	48.9	Stn242	5.2	0.164	-0.010	-0.191	5.9
Tooth Plate Area	7	43.6	Stn79	8.7	-0.219	0.032	0.237	10.5
Tooth Plate Area	21	2.9	Stn222	11.9	-0.268	-0.005	0.293	14.7

For each QTL, Linkage Group (LG), genetic position in centimorgans (cM), non-interpolated peak marker name, peak LOD score, mean size-corrected residuals of phenotypic values for Marine homozygotes (MM), Marine-Benthic heterozygotes (MB), and Benthic homozygotes (BB), and percent variance explained (PVE) among the F2s are shown.

**Table S5. Chromosome 21 microsatellites used for fine mapping**

Stn Marker	Forward primer sequence (5' to 3')	Reverse primer sequence (5' to 3')	5' fluorophore	Accession number
Stn484	TGCAAAGCAAGTGTAACGAA	CTTCCCTTTGTCCGTTCT	FAM	Pr032250564
Stn485	AGCAGGTGAAAGTGTGTATAACG	AGGGCACTATGGTTTCACAGG	FAM	Pr032250565
Stn486	CACAAGCCTTTGTGTTGGTG	GAAACGGGATTCTTTGACCA	NED	Pr032250566
Stn487	CACGGCAAACAGGTGAGAC	TCGATGGGCTGTAAATCCTC	NED	Pr032250567
Stn488	AATTACACTGCCTGCACTTGG	GTCAGATGGACGGACAGACG	NED	Pr032250568
Stn489	AGTGACGAATCCCTCTTCTGC	CACACCTTGTTGTGTTTGTAGC	FAM	Pr032250569
Stn490	ATGAGGTCACCCTGCCTAAC	CGCCTGTCATATACACATTGC	FAM	Pr032250570
Stn491	AACGTTAACCAGTTGCAGTCC	GATGTCGACACAGAATCTCTTAGC	HEX	Pr032250571
Stn492	CCGTATGCAGCCTGTTGG	AACCTGACCCTCCTCTGACC	FAM	Pr032250572
Stn493	ACGCCTTCCTCGATCAGACC	TTGTTACGCGTTTCGTAGAGC	FAM	Pr032250573
Stn494	CTCTACTGCGCACGCTTAGG	GTCACATTTCTCGGTTTGC	FAM	Pr032250574
Stn426	TTCCTCTTCTCACAGGCTGA	CCTTTGATCCGCACAGTCA	FAM	Pr032250575

Primer sequences of new Stn microsatellite markers used for tooth QTL fine mapping. All forward primers were directly labeled with 5' fluorophores of FAM or HEX (IDT) or NED (ABI). Accession numbers in ProbeDB for each marker are listed.

## Supplementary Figures

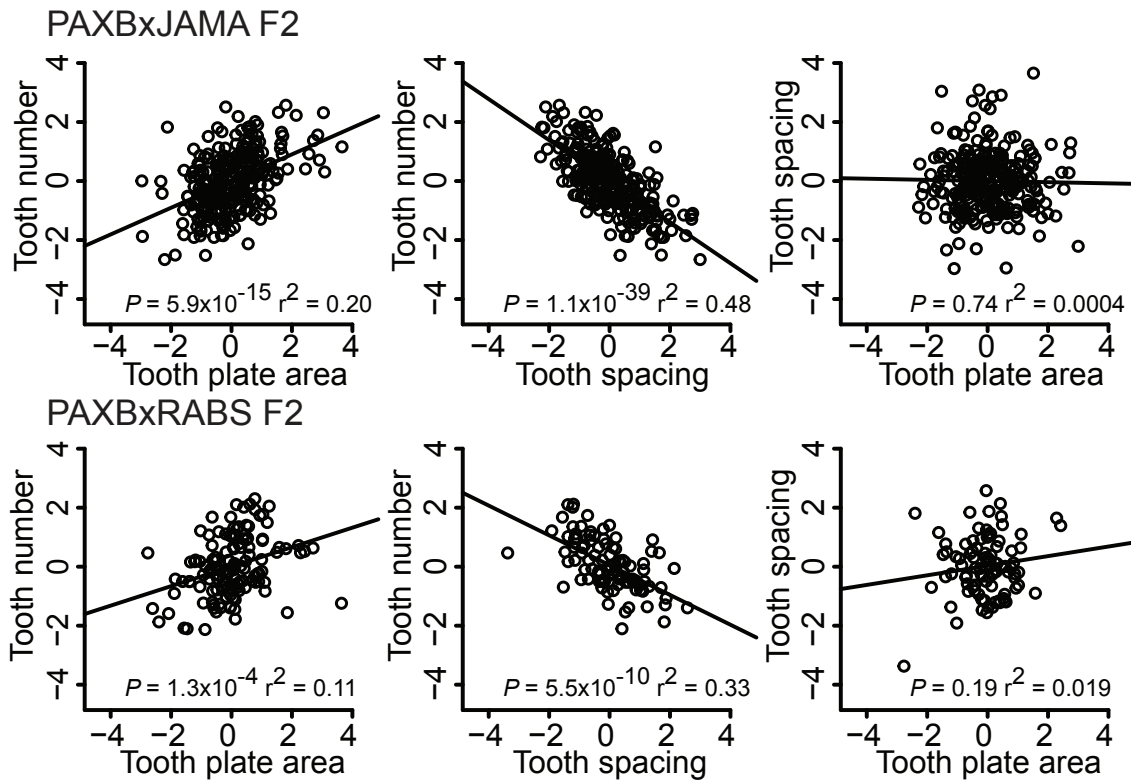


**Figure S1. Correlations of tooth number, area, and spacing in two F2 genetic crosses**

Pair-wise linear relationships for tooth number, tooth plate area, and tooth spacing for 272 fish from a Paxton benthic x Japanese Marine (top) and 142 fish from a Paxton benthic x Rabbit Slough Alaskan marine (bottom) F2 cross. Tooth number is significantly correlated with tooth plate area (left) and anti-correlated with tooth spacing (middle), suggesting that both area and spacing impact final tooth number. Conversely, tooth plate area and tooth spacing (right) are not correlated, suggesting that, despite each having an effect on total number, tooth plate area and spacing are genetically separable. The effect of fish length on each trait was removed using a linear regression and the residuals were z-scored in R. The  $P$  values ( $P$ ) and  $r^2$  values are shown for each comparison.

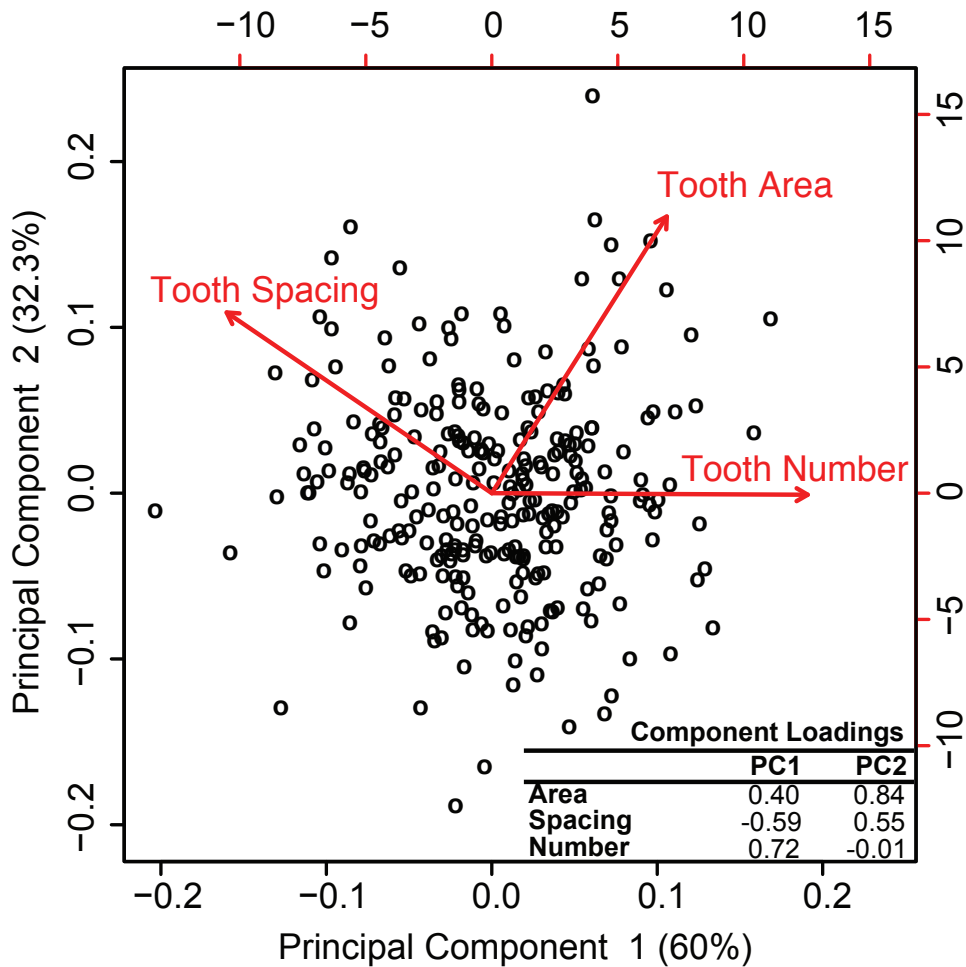


**Figure S2. Biplot of principal component analysis of tooth patterning phenotypes**

Scatter plot of the first two principal components from a principal component analysis of size-corrected tooth number, tooth plate area, and spacing phenotypes from 272 benthic by marine F2 fish. The first principal component (PC1) is explained primarily by variance in tooth number. Tooth area and spacing load orthogonally on PC1, suggesting genetic separability of area and spacing. The second principal component is explained largely by area and spacing with area loading stronger. Variable loadings are plotted for each trait in red and are presented in the inset. Percent variance explained is listed for each principal component on the axes.

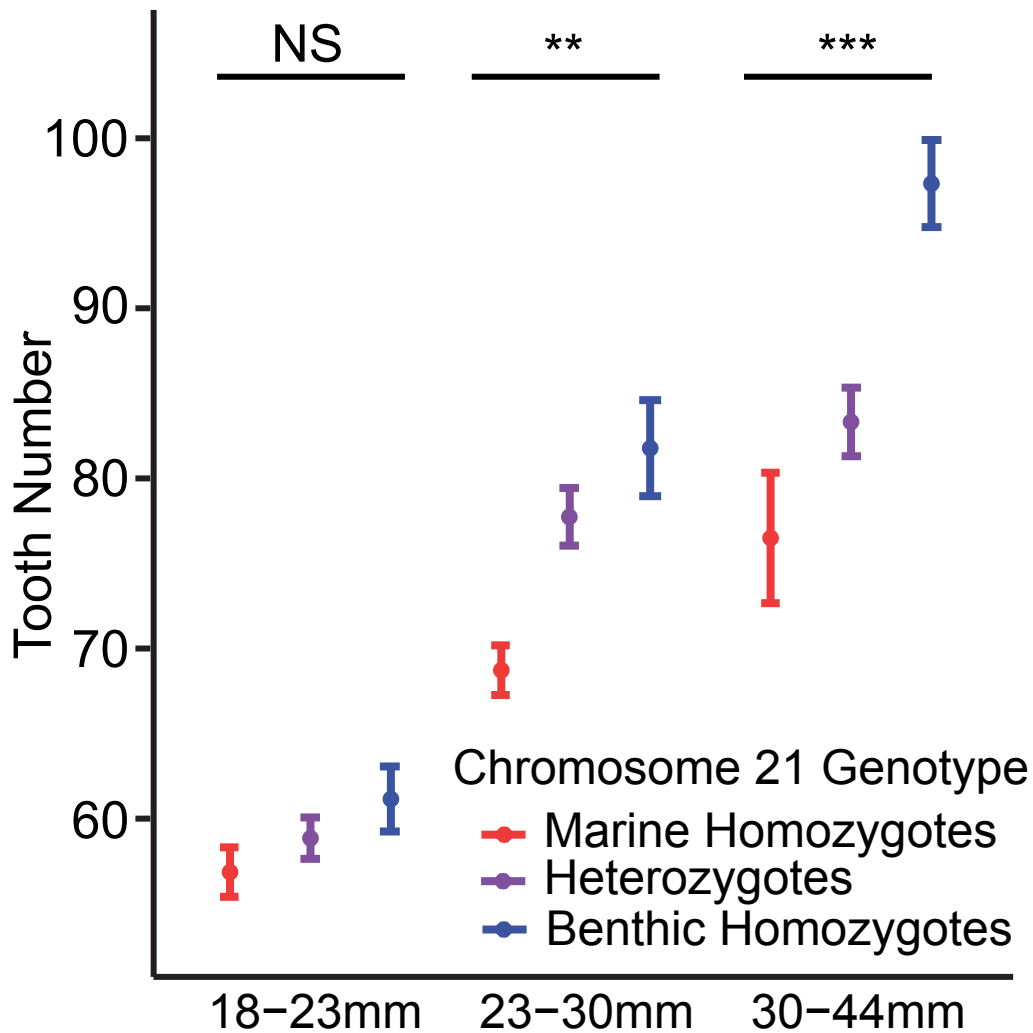


**Figure S3. Developmental effects of the chromosome 21 tooth QTL**

Effects of peak marker genotype on total tooth number (y-axis) in PAXB x RABS F2s at three different developmental time points (x-axis). The mean phenotypic value is shown for each genotypic class: marine homozygotes (red) heterozygotes (purple), and benthic homozygotes (blue). The effect of the QTL is not significant at the early larval time point, however at the later time points chromosome 21 genotype has significant effects on tooth number. The *P* values from a one-way ANOVA for each group are 0.32, 0.002, 0.0003, respectively. Error bars are standard error of the mean. Fish size is total length in millimeters (mm).

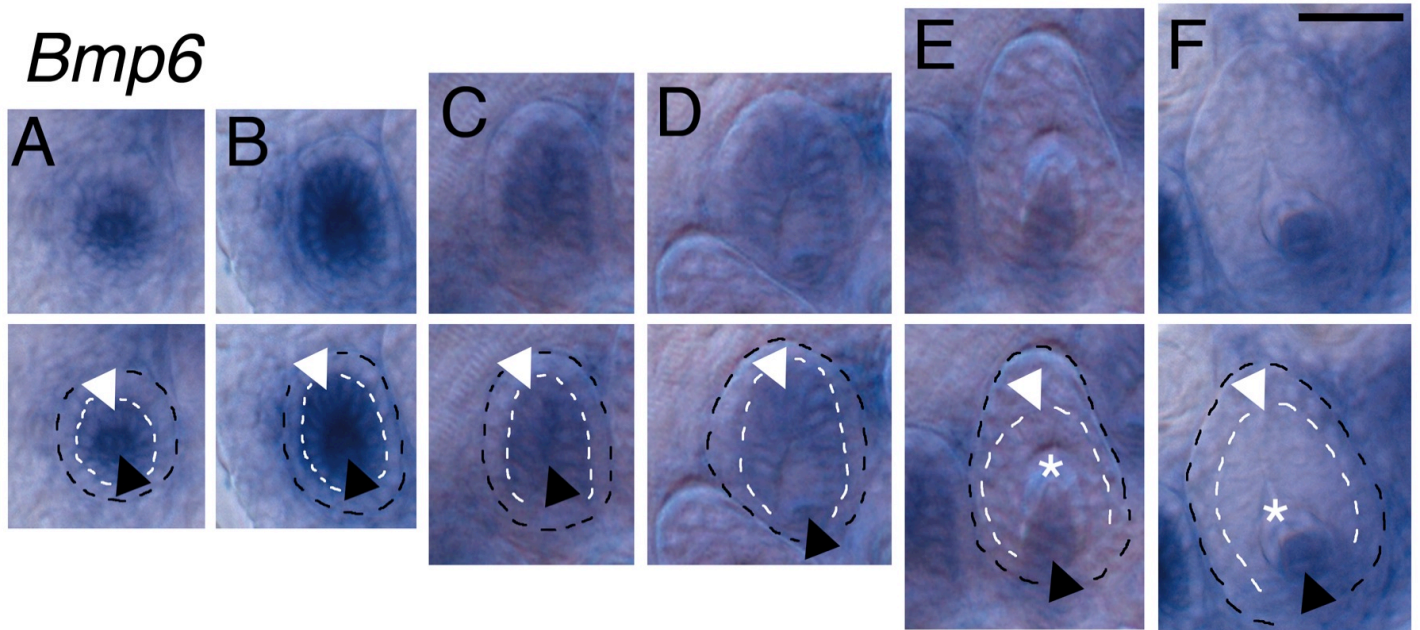


**Figure S4. Dynamic *Bmp6* expression in developing teeth.** Successive stages of tooth development from left to right, showing early germ stage (A) through newly mineralized baby tooth (F). Unlabeled images at top, and labeled versions below. As the pharyngeal tooth field has multiple germs forming at different stages (see Fig. 5G-H), example germs of different developmental stages from benthic fish 7.5-15 dpf are shown. In early germs (A), *Bmp6* expression is detected in inner dental epithelium (white arrowhead), and a rosette of odontogenic mesenchyme (black arrowhead). No expression is detected in the outer dental epithelium (area between white and black dotted lines). Slightly later in development (B-D), the tooth germ elongates and strong *Bmp6* expression is detected in the inner but not outer dental epithelium. As mineralization begins (E) and a baby tooth is formed (F), *Bmp6* expression is maintained in odontogenic mesenchyme, but is no longer detected in epithelia. For all germs, the black dashed line outlines the tooth germ, and the white dashed line outlines the boundary between the outer and inner dental epithelium. White arrowheads: inner odontogenic dental epithelium, asterisks: newly mineralized developing teeth, black arrowheads: odontogenic mesenchyme. Scale bar = 25  $\mu$ m.

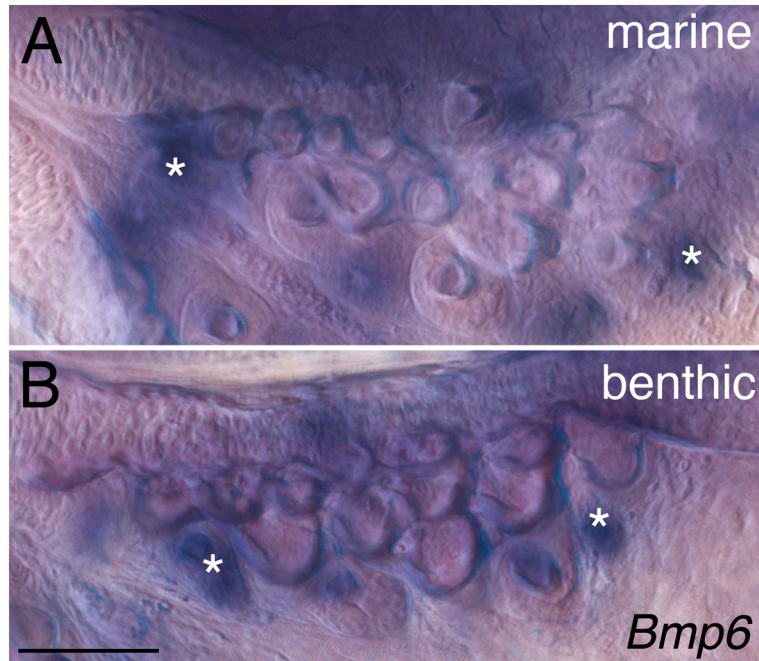


**Figure S5. *Bmp6* expression during larval tooth development**

In situ hybridization detecting *Bmp6* expression in developing pharyngeal teeth from (A) RABS marine and (B) PAXB benthic 30 day old (~10 mm total length) juvenile fish. *Bmp6* expression is detected in developing tooth germs (white asterisks). Scale bar = 100  $\mu$ m.

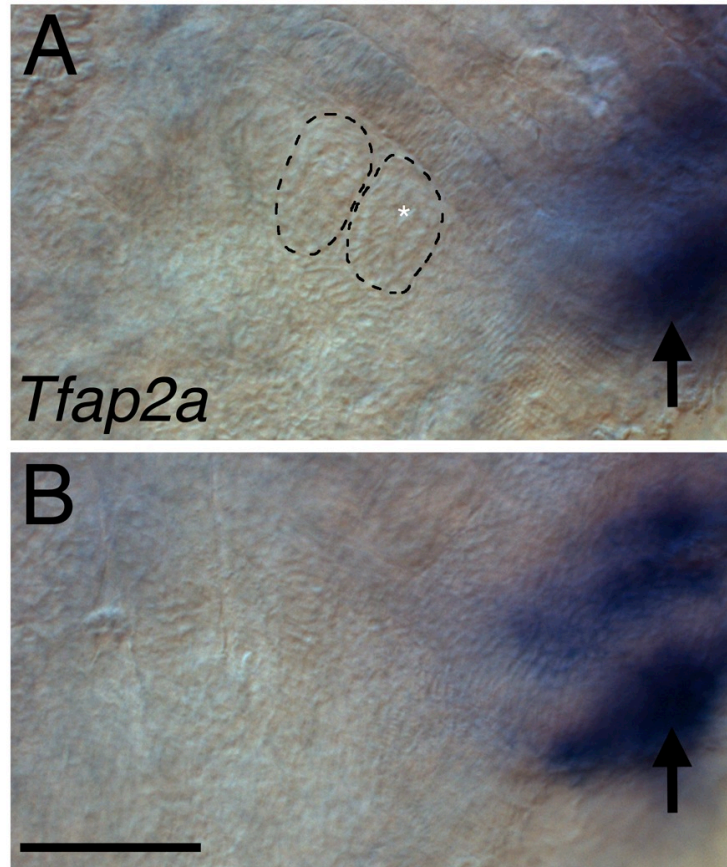


**Figure S6.** Expression of *Tfp2a* in 7.5 days post fertilization benthic fish. No *Tfp2a* expression was detected in developing stickleback tooth germs (A), although robust expression was detected in mesenchymal cells associated with the developing epibranchial cartilages. Shown are two focal planes, focused on (A) pharyngeal tooth germs and (B) dorsal pharyngeal mesenchyme (black arrow). In (A), two developing tooth germs are outlined with the black dashed lines, and a newly formed mineralized tooth is marked with the white asterisk. Scale bar = 50  $\mu\text{m}$ .

```

GaBMP6_PAXB MNSCWALVGLWWTAYCCMFLVAGSNYSLDGNNEVHPGFIHRRLRTHEKREMOKEILSIL
GaBMP6_JAMA MNSCWALVGLWWTAYCCMFLVAGSNYSLDGNNEVHPGFIHRRLRTHEKREMOKEILSIL
GaBMP6_RABS MNSCWALVGLWWTAYCCMFLVAGSNYSLDGNNEVHPGFIHRRLRTHEKREMOKEILSIL
DreBMP6 MTSALWFLSLFLWSCC-----LAGSSSVLDG-FLQSNFIHRRLRSEKREMOKEILSIL
OlaBMP6 MTSLLLALLGLCLSAVCVFT-AGSFSVDGNFEAAGFMHRRLRTHEKREMOKEILSVL

GaBMP6_PAXB GLPHRRPFPHPGKYNAPLFMLDLYNTISNEEKSRVEGIVDRIEPMQTPSPSLATYOE
GaBMP6_JAMA GLPHRRPFPHPGKYNAPLFMLDLYNTISNEEKSRVEGIVDRIEPMQTPSPSLATYOE
GaBMP6_RABS GLPHRRPFPHPGKYNAPLFMLDLYNTISNEEKSRVEGIVDRIEPMQTPSPSLATYOE
DreBMP6 GLNHRPFPHLNSGKYNAPLFMLDLYNMSSTEKSD---VDQYRSLFTTRPALASHHD
OlaBMP6 GLPHRRPFPHLNSGKYNAPLFMLDLYNTISSEDKS---QFLDRIYPSMRTTQSPPLATDOE

GaBMP6_PAXB SAFLNDADMVMSFVNLYEYDRELSPORRHHKEFKFNLSQIPEGEAVTAAEFRLYKECVSR
GaBMP6_JAMA SAFLNDADMVMSFVNLYEYDRELSPORRHHKEFKFNLSQIPEGEAVTAAEFRLYKECVSR
GaBMP6_RABS SAFLNDADMVMSFVNLYEYDRELSPORRHHKEFKFNLSQIPEGEAVTAAEFRLYKECVSR
DreBMP6 TEFTHDADMVMSFVNLYEYDRELSPORRHHKEFKFNLSQIPEGEAVTAAEFRLYKECVTS
OlaBMP6 TAFLNDADMVMSFVNLYEYDRELSPORRHHKEFKFNLSQIPEGEAVTAAEFRLYKECVSG

GaBMP6_PAXB AFRNDTFLVKVYQVVKHEPHREADLFLLESRRLWASEEGWLEFDITATSNLWVMSPAHNL
GaBMP6_JAMA AFRNDTFLVKVYQVVKHEPHREADLFLLESRRLWASEEGWLEFDITATSNLWVMSPAHNL
GaBMP6_RABS AFRNDTFLVKVYQVVKHEPHREADLFLLESRRLWASEEGWLEFDITATSNLWVMSPAHNL
DreBMP6 AFRNTEFLLSVYQVVKHEPHRDADLFLLESRRLWASEEGWLEFDITATSNLWVMSPAHNL
OlaBMP6 AFRNTEFLVKVYQVVKHEPHREADLFLLESRRLWASEEGWLEFDITATSNLWVMSPAHNL

GaBMP6_PAXB GLOVSVETSGGRSISGKEAGLAGRDGALEKOPFMVAFFKVSEVHIRSARSAGGKRRQON
GaBMP6_JAMA GLOVSVETSGGRSISGKEAGLAGRDGALEKOPFMVAFFKVSEVHIRSARSAGGKRRQON
GaBMP6_RABS GLOVSVETSGGRSISGKEAGLAGRDGALEKOPFMVAFFKVSEVHIRSARSAGGKRRQON
DreBMP6 GLOVSVETSGGRSISGKEAGLAGRDGALEKOPFMVAFFKVSEVHIRSARSAGGKRRQON
OlaBMP6 GLOVSVETSGGRSISGKEAGLAGRDGALEKOPFMVAFFKVSEVHIRSARSAGGKRRQON

GaBMP6_PAXB RNRSTQPQDGSRGLGP-----ADYNSSDQKTACRRHELFSFRELGWQDWIIAPEGYAAN
GaBMP6_JAMA RNRSTQPQDGSRGLGP-----ADYNSSDQKTACRRHELFSFRELGWQDWIIAPEGYAAN
GaBMP6_RABS RNRSTQPQDGSRGLGP-----ADYNSSDQKTACRRHELFSFRELGWQDWIIAPEGYAAN
DreBMP6 RNRSNQPQDGSRGLGP-----ADYNSSDQKTACRRHELFSFRELGWQDWIIAPEGYAAN
OlaBMP6 RNRSTQPQDASRGSSLPVRETSADYNSSDQKTACRRHELFSFRELGWQDWIIAPEGYAAN

GaBMP6_PAXB YCDGECSPFLNAHMNATNHAI VQTLVHLMNPENVPKCCAPT KLHAI SVLYFDDNSNVIL
GaBMP6_JAMA YCDGECSPFLNAHMNATNHAI VQTLVHLMNPENVPKCCAPT KLHAI SVLYFDDNSNVIL
GaBMP6_RABS YCDGECSPFLNAHMNATNHAI VQTLVHLMNPENVPKCCAPT KLHAI SVLYFDDNSNVIL
DreBMP6 YCDGECSPFLNAHMNATNHAI VQTLVHLMNPENVPKCCAPT KLHAI SVLYFDDNSNVIL
OlaBMP6 YCDGECSPFLNAHMNATNHAI VQTLVHLMNPENVPKCCAPT KLHAI SVLYFDDNSNVIL

GaBMP6_PAXB KKYKNMVVRACGCH
GaBMP6_JAMA KKYKNMVVRACGCH
GaBMP6_RABS KKYKNMVVRACGCH
DreBMP6 KKYKNMVVRACGCH
OlaBMP6 KKYKNMVVRACGCH

```

**Figure S7. Predicted amino acid alignment of BMP6 in fish**

BMP6 sequences of Paxton benthic freshwater (GaBMP6\_PAXB), Japanese Pacific marine (GaBMP6\_JAMA), and Rabbit Slough Alaskan marine (GaBMP6\_RABS) are shown aligned to the BMP6 sequences of Zebrafish (DreBMP6) (Genbank accession number = NM\_001013339.1) and Medaka (OlaBMP6) (Ensembl ENSORLT0000008205). Stickleback intron/exon boundaries are marked with arrowheads. The asterisk marks the position of the synonymous SNP used for the pyrosequencing assay. The predicted amino acid sequence is identical across the three stickleback populations.